

NASA Technical Memorandum 83781

Structural Design of a Vertical Antenna Boresight 18.3- by 18.3-m Planar Near- Field Antenna Measurement System

G. Richard Sharp, Paul A. Trimarchi,
and Joyce S. Wanhainen
*Lewis Research Center
Cleveland, Ohio*

Prepared for the
Meeting of the Antenna Measurement Techniques Association
San Diego, California, October 2-4, 1984

NASA

STRUCTURAL DESIGN OF A VERTICAL ANTENNA
BORESIGHT 18.3- BY 18.3-m PLANAR NEAR-FIELD
ANTENNA MEASUREMENT SYSTEM

G. Richard Sharp, Paul A. Trimarchi, and Joyce S. Wanhainen
National Aeronautics and Space Administration
Lewis Research Center
Cleveland, Ohio 44135

INTRODUCTION

The near-field antenna testing technique is now an established testing approach. It is based on the work done over a twenty-year period by the National Bureau of Standards (Boulder, Colorado), the Georgia Institute of Technology and others. The near-field technique is used for large aperture, high frequency antennas where the antenna to probe separation necessary to test in the far-field of the antenna is prohibitively large.

Studies have been conducted to identify the testing requirements for advanced communications spacecraft antennas and antenna research. Based on these studies and recent trends in spacecraft antenna development, the need was identified for a system to test large high frequency antennas.

When these large, high frequency, delicate, space based antennas are to be tested on the ground, near-field testing becomes the only plausible test method. If the planar near-field approach is used and the scan area is large enough, the antenna does not have to be moved during testing. Thus, for space based antennas, compensation for antenna sag in one g becomes a matter of properly supporting the antenna to best approximate its zero g shape. This can best be done with the antenna boresight vertical for most large antennas now contemplated.

A planar scanner with a 18.3 m by 18.3 m (60 ft by 60 ft) horizontal scan plane was chosen for this design study. The scanner was configured so that the height of the horizontal scan

plane could be adjusted to accommodate various sized antennas. These antennas can then be simply and rigidly supported on a concrete floor to best simulate their zero g shape.

This report describes the results of parametric studies that optimize the scanner structures regarding deflection caused by the live load at the scan plane. The resulting structure was then analyzed to determine its dynamic response. This response data will be used in the design of the scanner motion control system.

With this scanner configuration and its relatively stiff structure, it will be possible to meet the critical vertical deflection criteria (at 60 GHz) of the RF probe tip that defines the actual scan plane. This will be accomplished by adjusting rail heights to compensate for the relatively small vertical deflection caused by the probe cart and traveling beam horizontal movements.

The purpose of this report is to document the results of the structural and dynamic analysis for a large scanner needed to support future antenna testing requirements. This report can also be considered a data base for the design of other similar large structures whether they be designed for near-field antenna testing or other purposes (i.e., testing large parabolic solar power collectors).

SCANNER CONFIGURATION AND DESIGN REQUIREMENTS

Scanner Configuration

Large, lightweight space type antenna reflectors, such as the Harris Hoop-column [1] or the Lockheed wrapped-rib [1] must be adequately supported when tested in a one g environment so their shape in the zero g environment is simulated. If these reflectors were mounted with the antenna boresights horizontal, the reflectors would sag. This sag would be difficult to control because varying horizontal tensile and compression forces would be needed to bring the reflector back to its zero g shape. Also, this adjustment work would need to be done over the full

height of the diameter of the antenna. However, if the reflector can be mounted with the antenna boresight vertical, simple ceiling mounted or floor mounted jack posts can be used for antenna shape adjustment.

If the antenna were mounted from the "ceiling" (aiming downward), workers would be required to measure and adjust the antenna from its ceiling mounted position. Then if the "ceiling" moved, errors would result. Therefore, the "ceiling" could not be attached to the building but would be comprised of a rigid platform supported from separate posts. In light of this, the decision was made to mount the antenna on the floor both for the ease of zero g compensation and for the safety, convenience and expediency of the technicians. On the floor, the antenna does not have to be moved in any way.

With the antenna mounted on the floor facing upward, a structure was needed to provide for motion of a probe (or probes) over a flat horizontal plane at various heights from the floor (to accommodate various height antennas). Vertical out of scan plane motion of the probe tip during scanning would result in phase errors in the recorded data. Therefore, the structure carrying the probe had to be very rigid or else a phase error compensation scheme would be needed. The most prudent path was to make the probe carrying platform rigid. This should make the phase error compensation scheme simpler if it is needed at all.

The resulting scanner configuration (fig. 1) consists of a movable support frame that can be adjusted in height to compensate for varying antenna configurations. This support frame is guided in its vertical motion by rails on the corner towers of the outer support structure. A cable-counterweight system is used to support the weight of the movable platform. The counterweight carts travel inside the outer support structure towers. A traveling beam moves on five rails attached to the movable platform for probe motion in the X horizontal direction. Probe motion in the Y direction is given by a probe carrying cart that travels on rails attached to the traveling

beam. RF absorber material must be attached to the lower faces of the movable support frame, traveling beam and probe cart or carts to prevent RF energy reflection and resultant errors.

A 1/24 scale model of the 18.3 m by 18.3 m (60 ft by 60 ft) planar near-field antenna scanner has been constructed. Figure 2 shows the model displayed on a table representing the floor plan of the proposed Antenna Technology Laboratory. A model (to the same scale) of the operational 6.7 m by 6.7 m (22 ft by 22 ft) planar near-field antenna scanner is shown next to the large scanner [2].

Structural Design Requirements

The criteria for the structural design are that: 1. The structure be of sufficient stiffness that the Z-axis deflections caused by the static loads of the probe cart(s) and the traveling beam be easily compensated for by precambering (curving upward between support points) the rails on which they travel; 2. The structure be rigid such that it not resonate (react adversely dynamically) to the moving loads caused by the desired motions of the probe cart and traveling beam; and 3. The structure be low in cost.

During near-field testing, it is essential that the scan plane (Z-axis motion of the probe tip (or probe tips)) not exceed (RF wavelength)/100. If this is not possible, it is essential that the Z-axis motion be known so that either compensating corrections can be made in the RF phase data or an open loop Z-axis probe motion control system used. At the desired test frequency of 60 GHz this wavelength/100 criteria means that the scan plane (probe tip motion in the Z direction) would need to be flat within 0.051 mm (0.002 in) rms. This can be accomplished by designing a relatively stiff 2.59 m (8.5 ft deep) movable support frame and then compensating for the remaining deflection by arcing or precambering the rails that the traveling beam rides such that the beam motion is as flat as reasonably possible. The Z-axis motion of the probe tip while moving along the traveling beam can be compensated for in a like manner.

When the probe cart or traveling beam is started or stopped, it is essential that the entire support structure react in a predictable manner and not react dynamically or couple with these motions. These motions can be separated or uncoupled if the natural frequencies (rigid body and flexible body modes) of the various structural parts are at least double the excitation frequency. The excitation vibration or shock impulse comes from the acceleration of the probe cart or traveling beam to the constant scan velocity. Therefore, the acceleration period for each of these masses during testing must be at least twice the time it takes for the lowest frequency resonant mass of the scanner to complete one fourth of a cycle in order to limit dynamic coupling. However, the entire structure must still resist the uncoupled acceleration forces in order to prevent errors in the known versus perceived location of the probe tip in the X-Y plane. The allowable X or Y deflection is 0.051 mm (0.002 in.) in order not to exceed (RF wavelength/100) criteria at 60 GHz.

It is important that the cost of the structure be kept low. For this reason, the primary structures of the scanner are comprised of standard steel sections. Welding was chosen for the steel joining technique so that the structures and especially the joints can be kept simple. It is believed that these steps will allow the main steel structural assemblies and sub-assemblies to be factory fabricated rather than assembled in the field, thus affecting large cost savings.

The weight of the structural parts should be minimized both to reduce cost and to minimize the dynamic masses of the moving elements. Smaller dynamic masses will result in higher structural natural frequencies and will ease the dynamic controls problem.

Thermal Design Requirements

A simple check of the thermal expansion of a steel column 20 m (60 ft) tall indicated a growth of approximately 230 μm (0.0091 in.) for a 1° C temperature rise. The total allowable

Z-axis dimensional discrepancy at 60 GHz would be 50 μm (0.002 in.) rms. Thus, accurate temperature control of the test cell or of the column itself will be required within specific limits, possibly $\pm 0.1^\circ\text{C}$. If this proves too difficult, laser interferometer controlled closed loop height adjusters will be required at each corner of the movable support frame. A thermal gradient between the floor and ceiling of the test cell could be tolerated only if it is uniform across the horizontal plane of the test cell.

NASTRAN ANALYSIS

The NASTRAN analyses were undertaken in order to optimize the scanner's structural design and to predict its static and dynamic behavior. The approach used for this analysis was to perform a static analysis on the original scanner design and then optimize its parameters while still maintaining the design requirements. A dynamic analysis was then performed on the optimized static structural design to assure that it met the dynamic design requirements. All segments of the NASTRAN analysis were checked with point design calculations.

Structural Optimization

Model Description

NASTRAN static analyses were performed on the scanner structure to aid in providing a preliminary design and then to optimize structural member sizes at acceptable deflections. This later parametric static analysis optimized the size of the structural members in the critical moving assemblies: the movable support frame and the traveling beam. Parametric analysis of the outer structure was not considered necessary because it is not deflection or weight critical regarding the scanning plane static analysis.

Each interconnection between members of the structure was modeled as a rigid joint. The joint locations were entered in the NASTRAN program with NASTRAN GRID cards.

The structural members were modeled by straight, prismatic CBAR elements connecting the grid points. CBAR elements have extensional and torsional stiffness; they also have bending stiffness and transverse shear flexibility in two perpendicular directions. First, truss geometries were chosen for the movable support frame and traveling beam. Then, the member sizes and truss heights were optimized to yield minimal static deflection under normal operating loads.

A series of point design calculations were performed on small simplified segments of the traveling beam and movable support frame. These calculations used the method of unit loads to verify the order of magnitude of the NASTRAN deflections.

Movable Support Frame

The movable support frame was analyzed by constraining its four corners in space through the use of single point constraint (SPC) cards. The first corner was constrained in all three translational directions (x, y, and z). A second adjacent corner was fixed in two directions (x and z (vertical)); and the remaining two corners were fixed in the 'z' direction only.

The loads, represented by FORCE cards, were applied at points that simulated the weight of the traveling beam, cart, and the RF absorbent material. Loads representing the traveling beam were located in a line at the middle of the movable support frame. The loads representing the cart were centrally located on the traveling beam.

The movable support frame is a welded structure fabricated from structural steel angles and tees. Table I summarizes the initial choice of materials for the frame used in this analysis. The (resulting) NASTRAN generated model of the movable support frame is shown in Fig. 3.

In the parametric optimization analysis, the frame height and the size of the structural tees (longerons) of the movable support frame were systematically decreased. Figure 4 is a plot

of the maximum support frame vertical deflection versus the support frame height for longerons of decreasing size. Note that for a fixed moveable support frame height, the maximum deflection remains relatively constant as a function of the structural size of the upper and lower frame longerons. From this parametric analysis, the structural tee ST12WF (74.4 kg/m) (50 lb/ft) was chosen as optimum because it provided adequate frame rigidity and also was the lightest available member to meet the minimum tee flange width requirements. The analysis also indicated that the relatively small height of 2.13 m (7 ft) would provide adequate rigidity. However, the height of 2.59 m (8-1/2 ft) was chosen because it not only reduced weight, cost, and deflection, but also provided adequate head room for maintenance personnel walking inside the frame structure. The resulting optimized member sizes for the movable support frame are summarized in Table II.

Traveling Beam

The design goal for the traveling beam was to minimize overall beam height, beam weight and beam deflection between support points. The traveling beam was analyzed using loads representing the RF absorbent material, the probe cart, and the probe cart guide rails. For the computer model (fig. 5), the traveling beam was suspended by its rail support struts. The ends of the rail support struts were assumed simply supported in space. Three traveling beam heights and five truss member size groups were analyzed. The results of the static analysis are summarized in Table III.

The design goal for both the movable support frame and the traveling beam was to minimize overall structural height and thus maximize the overall working height. Therefore, 0.91 m (3 ft) was chosen for the height for the traveling beam. The truss member size combination that was chosen, while not the lowest in weight or the stiffest, yielded an overall truss weight of 1896 kg (4180 lb) while holding the deflection to only 0.787 mm (0.031 in.). This conservative choice will allow the

use of heavier instrumentation or possibly multiple carts in the future if needed.

NASTRAN Static Results

Deflection of the movable support frame due to the live loads of the traveling beam and probe cart was studied by analytically modeling the cart and traveling beam in four different positions (fig. 6) and then comparing the resultant deflections. The 2.59 m (8-1/2 ft) high movable support frame showed a deflection ranging from 0.41 to 1.02 mm (0.016 to 0.040 in.) at the four chosen cart positions. A similar analysis of deflection due to the live load of the probe cart only was conducted for the traveling beam. The traveling beam (with the optimized height and member size) yielded a maximum deflection of 0.14 mm (0.0056 in.) between support points. Deflection due to the probe cart and traveling beam live loads will be adjusted out of the system. This will be accomplished by precambering upward the support rails on the movable support frame and traveling beam to compensate for local rail and structural deflection caused by the moving components.

Dynamic Analysis

The purpose of the dynamic analysis was to determine the vibration modes and natural frequencies of the scanner structure. This information will be used for designing a drive system for the probe cart and traveling beam that will not couple dynamically with the scanner natural frequencies.

Model Description

The model used for the scanner dynamic analysis linked all the major components in the scanner. The movable support frame was attached to the four outer support frame towers in a manner that simulated the connections of the support frame riding on vertical guide rails. The support frame attachments to the vertical guide rails were modeled with elastic elements (CELAS2). The spring rates used in these elements represented the lateral stiffness of the bearings, rails, and the rail supports under

bending and torsional loads. Figure 7 shows these elastic element connections.

The support frame is held vertically (in the Z-axis) by cables attached to counterweights riding in the outer frame vertical towers. The support frame is positioned vertically by a continuous chain vertical drive mechanism. Counterweight cables and vertical drive chain connections to the movable support frame were modeled as one elastic element. The spring rates used in these elements represent the combined stiffness of the cable and chain under axial loading. Figure 8 shows these elastic element connections.

The traveling beam and probe cart attachments were modeled to simulate the connections of these components to their horizontal support rails and drive chains. These beam and cart links were also modeled with elastic elements (CELAS2). The spring rates used for the rail attachment elements represent the relative stiffness of the bearing, rails, and rail supports under bending and torsional loads. The spring rates (in line with the rails) that attach the traveling beam to the support frame or the cart to the beam represent the axial spring rate of the drive chain loops. All these elastic element connections are shown in Figs. 9 and 10.

For the dynamic model, all scanner structural elements were modeled by utilizing the individual static analysis models. The nonstructural masses such as the RF absorber, decking, bearings, etc., were represented on concentrated mass cards (CONM2). The static analysis loads were originally modeled with FORCE cards. However, this code had to be changed to CONM2 cards because the dynamic analysis recognizes only masses.

The attachment spring rates for the probe cart, traveling beam and movable support frame were determined from point design calculations. It was assumed that Thomson Series XR linear bearings and tubular 60 case hardened shafts were used on the guide rail systems. Morse 12.7 mm (1/2 in.) pitch 25.4 mm (1 in.) wide silent chain was used in the drive system. Three

25.4 mm (1 in.) steel cables were used to attach the movable support frame to the counterweights at each corner.

Each structural joint was modeled as a rigid joint as in the static analysis. The grid points at the bases of the columns in the outer support frame were constrained in three translational directions (x, y, and z), but left free to rotate about any axis. Figure 11 shows the NASTRAN generated model of the total structure.

Dynamic Analysis Check

The lowest natural frequencies to be found should be the rigid body modes of the movable support frame. For these modes, the movable support frame should have independent movements about each translational and rotational axis. These low frequency modes are the most critical because they will affect the drive system dynamic requirements. The frequencies for each of these modes have been hand calculated to serve as a check on our NASTRAN model.

NASTRAN Dynamic Results

As predicted in the dynamic analysis check, the first six vibration modes were the six degree of freedom rigid body motions of the movable support frame with some coupling to the traveling beam and the outer support structure at the higher frequencies. The motions of each of these modes are described in Table IV. Figures 12 to 17 show NASTRAN plots of and give natural frequencies of the movable support frame rigid body modes.

The minimum acceleration time required for any of the moving components of the scanner to reach the constant scan velocity of 30 cm/sec (1 ft/sec) depends on the allowable reaction movement of the supporting structure. This movement is amplified by up to a factor of two if the acceleration period and the supporting structure natural frequency are identical. In order to greatly limit dynamic coupling between the drive system and the scanner structure, this acceleration time must be twice the time it takes for the structure to complete 1/4 of a cycle at its lowest

natural frequency. The NASTRAN analysis found the lowest frequency to be 1.17 Hz. The period for this natural frequency is 0.85 sec. Thus the minimum constant acceleration time allowed would be 0.42 sec. This acceleration time will result in near zero dynamic coupling. The deflection of the movable support frame relative to the ground when the traveling beam is accelerated is 0.0043 mm (0.00017 in.). The deflection of the movable support frame/traveling beam system when the probe unit is accelerated is 0.0051 mm (0.00020 in.). Both these deflections are considerably less than the 0.051 mm (0.002 in.) position error allowable at 60 GHz.

CONCLUSIONS

A NASTRAN static and dynamic structural analysis of the proposed 18.3 m by 18.3 m Planar Near Field Scanner has been completed. During this analysis, critical vertical deflections at the RF probe tip and overall deflections were computed. The structure of both the movable support frame and the traveling beam were optimized so that the static deflection criteria for these structures could be met at near minimum weight and cost. When the static deflection criteria had been satisfied, the entire structure was analyzed dynamically to ascertain the lowest frequency dynamic responses. The results of all of these analyses were highly satisfactory demonstrating the feasibility of the design concept.

At a given constant temperature, the static deflection criteria depend on the ability of the rail adjustment system to compensate for the vertical deflection. This is accomplished by precambering the rails (arcing the rails upward) between structural hard points. The static deflection goals that would allow this type of rail adjustment have been met.

Both the movable support frame and traveling beam structures have been optimized regarding the trade between vertical static deflection and the weight of the structures in question. One interesting result is that for a fixed movable support frame height, the maximum deflection remains relatively constant as a

function of the structural size of the upper and lower frame longerons. Thus, it was possible to reduce the weight (and cost) of these members by 43 percent compared to the original estimates while holding the maximum static deflection relatively constant at a fixed frame height. The traveling beam structure was also optimized. However, in the case of the traveling beam, the maximum truss deflection was governed by the sizes of the upper and lower truss members and was less dependent on truss depth. However, the cross-sectional area (and weight) of the truss diagonals did have a large effect. It was found that for a fixed traveling beam truss depth and fixed upper and lower truss member sizes, reducing the wall thickness of the diagonal tubes actually reduced the static deflection as a result of the accompanying truss weight reduction.

The first twelve modes of vibration of the entire structure have been calculated. As expected, the six lowest frequency modes were the six degree of freedom rigid body modes of the movable support frame with some traveling beam and outer structure coupling. Only in the higher modes does extensive coupling start to take place between the rigid body modes and flexible body modes of the structural components. These higher modes are of academic interest only since the primary concern (and reason) for the dynamic analysis is to eliminate coupling between the probe cart and traveling beam drive system dynamics and the lowest orthogonal or pitching structural vibration modes in any axis. The lowest natural frequencies calculated are high enough that the drive system designers should have little problem eliminating system coupling.

Many structural details remain to be designed. Toward this end, a 1/24 scale model of the scanner structure was built. It has been very helpful in designing joints between intersecting trusses and between individual truss members. However, the detail design of these joints remains to be done. Also, as the detail design is finalized, more accurate data will be needed on the localized spring rates at the structure/rail interfaces for all of the movable structural elements. When these data are

available, the dynamic analysis should be recomputed using these later values in order to ensure that no coupling exists between the drive systems and the structural vibration modes.

REFERENCES

1. Large Space Antenna Systems Technology - 1982 (NASA Conference Publication 2269).
2. "Characteristics and Capabilities of the Lewis Research Center High Precision 6.7 m by 6.7 m Planar Near-Field Scanner" by G. R. Sharp, R. J. Zakrajsh, R. R. Kunath, C. A. Raquet, and R. E. Alexovich (TM-83785).

**TABLE I. - MOVABLE SUPPORT FRAME MATERIALS
INITIAL CHOICE**

MEMBER	MATERIAL
LONGERONS	ST18WF Tee, 171.1 kg/m (115 lb/ft)
CROSS PIECES	152.4 x 152.4 x 9.53 mm angle (6 x 6 x 3/8 in)
DIAGONALS	152.4 x 152.4 x 9.53 mm angle (6 x 6 x 3/8 in)
END DIAGONALS	203.2 x 203.2 x 12.7 mm angle (8 x 8 x 1/2 in)
VERTICAL CORNER SUPP'TS	ST18WF Tee, 171.1 kg/m (115 lb/ft)

**TABLE II. - MOVABLE SUPPORT FRAME MATERIALS
OPTIMUM CHOICE**

MEMBER	MATERIAL
LONGERONS	ST12WF, 74.4 kg/m (50 lb/ft)
CROSS PIECES	152.4 x 152.4 x 9.53 mm angle (6 x 6 x 3/8 in)
DIAGONALS	152.4 x 152.4 x 9.53 mm angle (6 x 6 x 3/8 in)
END DIAGONALS	203.2 x 203.2 x 12.7 mm angle (8 x 8 x 1/2 in)
VERTICAL CORNER SUPP'TS	ST12WF, 74.4 kg/m (50 lb/ft)

TABLE III. - TRAVELING BEAM WEIGHT CALCULATIONS

Height, m	Size of members, mm	Total weight of members, kg	Weight reduction in traveling beam, %	Max. displacement, mm
1.219	101.6x101.6x6.35 (upper truss longeron)	3236	-	0.81
1.067	101.6x101.6x3.1 (lower truss longeron)	3039	6	.89
.9144	88.9x88.9x3.1 (truss diagonals)	2846	12	.94
1.219	76.2x76.2x6.35 (upper truss longeron)	2301	29	1.50
1.067	76.2x76.2x3.1 (lower truss longeron)	2161	33	1.63
.9144	6.35x6.35x3.1 (truss diagonals)	2026	37	1.75
1.219	101.6x101.6x6.35 (upper truss longeron)	2111	35	.660
1.067	101.6x101.6x3.1 (lower truss longeron)	2003	38	.711
.9144 (design choice)	88.9x88.9x1.58 (truss diagonals)	1896	41	.787
1.219	76.2x76.2x6.35 (upper truss longeron)	1516	53	1.24
1.067	76.2x76.2x3.1 (lower truss longeron)	1439	56	1.35
.9144	6.35x6.35x1.58 (truss diagonals)	1364	58	1.47

TABLE IV. - SUMMARY OF THE RIGID BODY MODES OF THE
MOVABLE SUPPORT FRAME

Figure no.	Vibration mode	Natural frequency, Hz	Mode description
12	1	1.17	Torsional mode of movable support frame about Z-Z axis. Outer support frame is stationary.
13	2	1.90	Lateral mode of movable support frame along X-X axis. Outer support frame is stationary.
14	3	2.07	Vertical mode of movable support frame along Z-Z axis. Outer support frame is stationary.
15	4	2.54	Lateral mode of movable and outer support frames along Y-Y axis. Pitching of movable support frame about X-X axis.
16	5	3.00	Pitching of movable support frame about X-X axis. Lateral mode of outer support frame along Y-Y axis.
17	6	3.08	Pitching of movable support frame about Y-Y axis coupled with lateral bending of the traveling beam on the X-Y plane. Lateral mode of outer support frame along X-X axis.

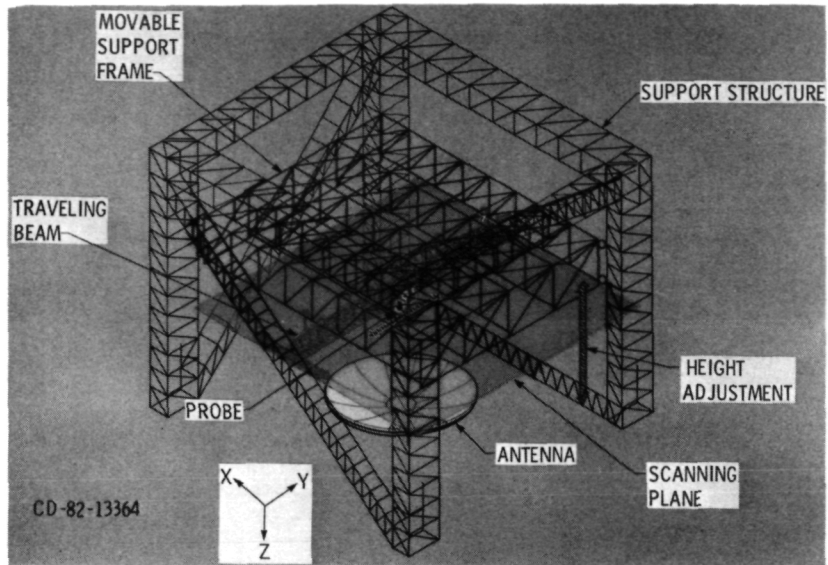


Figure 1. - 60' x 60' vertical boresight near-field planar scanner.

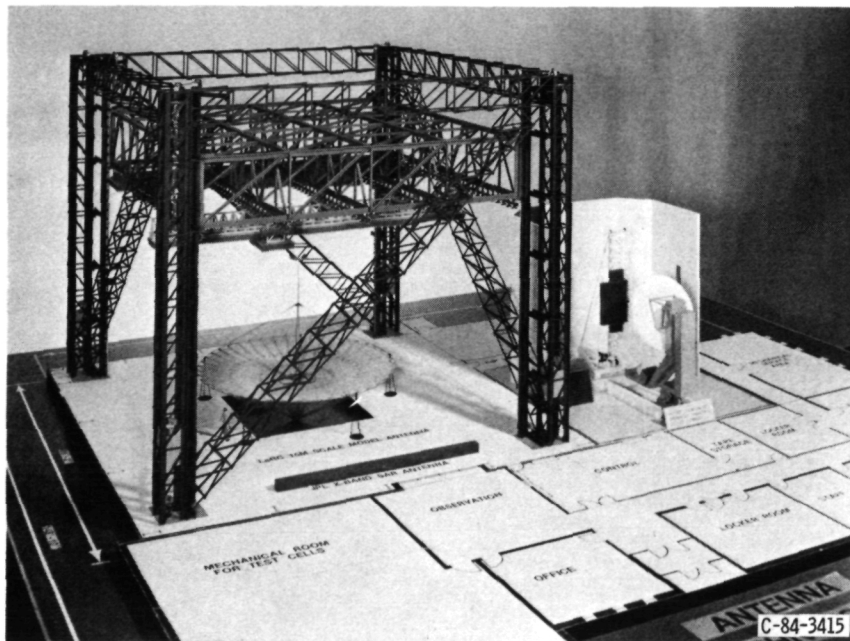


Figure 2. - 18.3 m X 18.3 m Planar near-field antenna, 1/24 scale model displayed on floor plan of proposed laboratory.

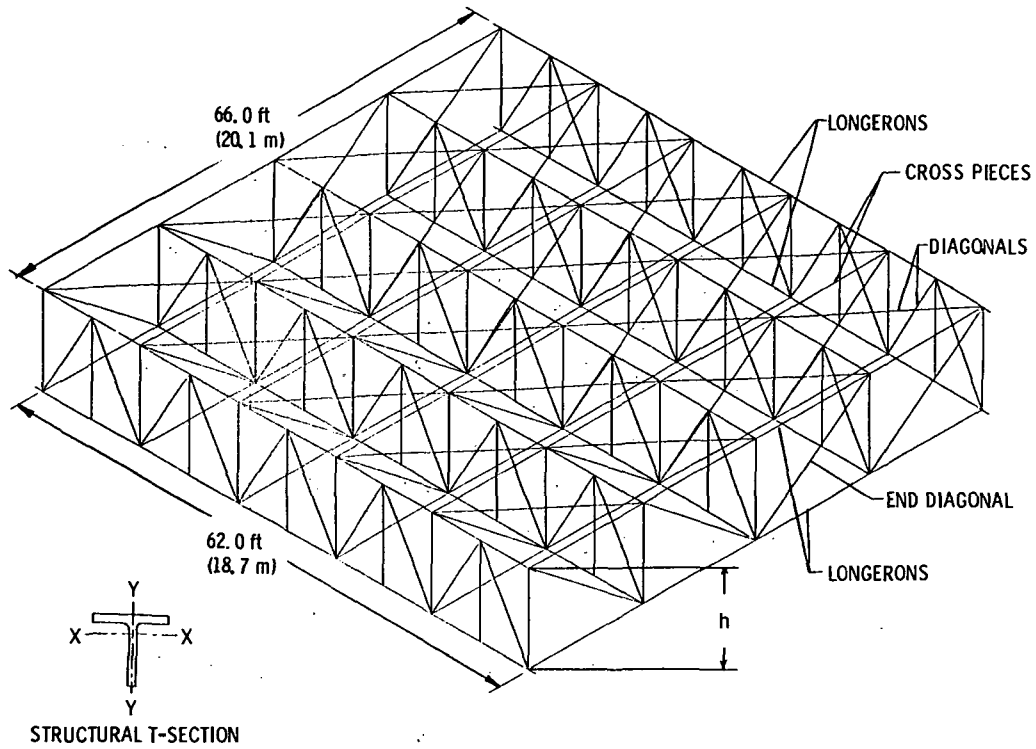


Figure 3. - Nastran model of movable support frame.

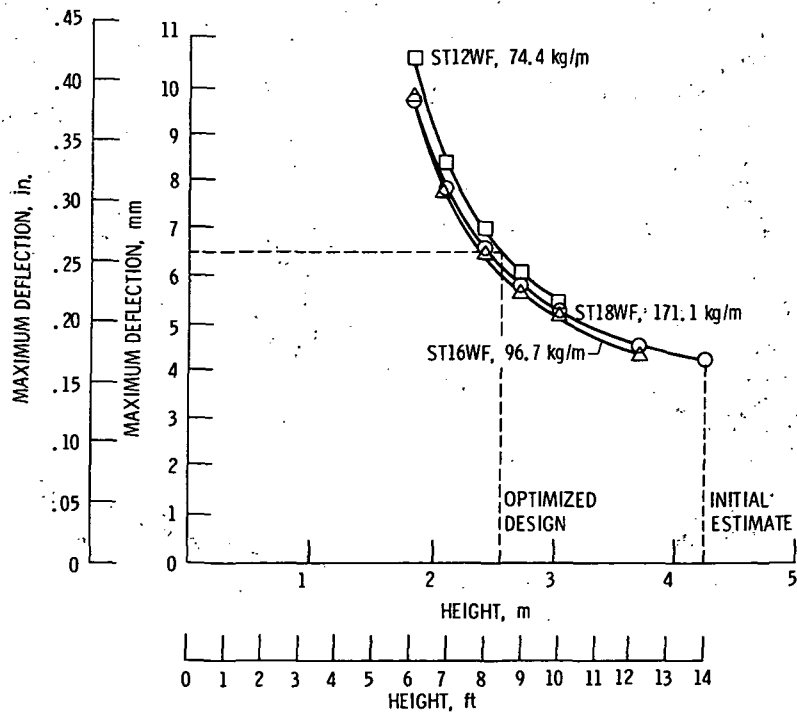


Figure 4. - Movable support frame, maximum deflection vs. height and T-section.

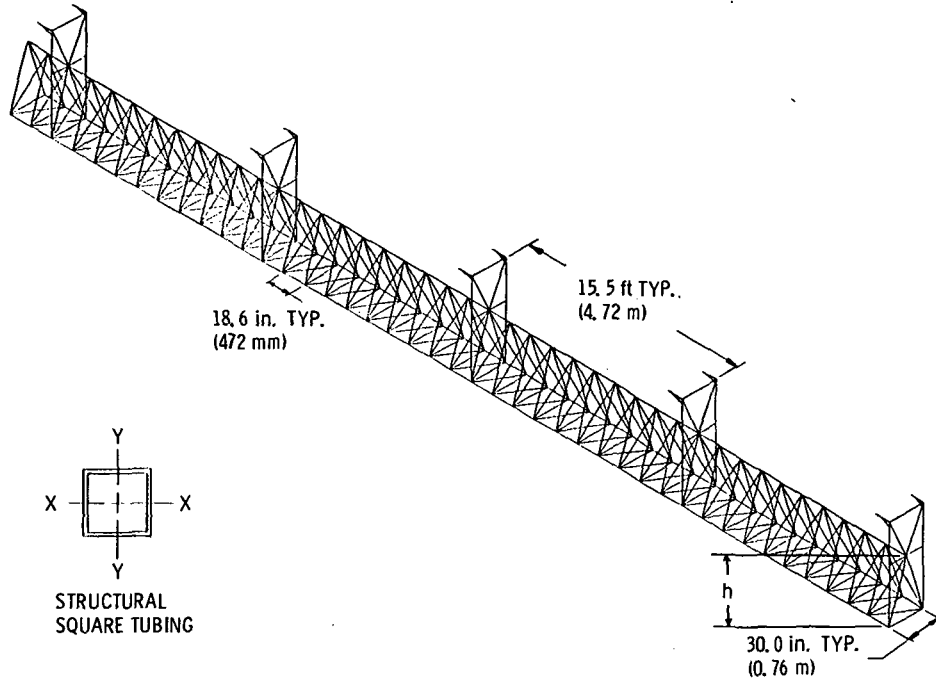


Figure 5. - NASTRAN model of traveling beam.

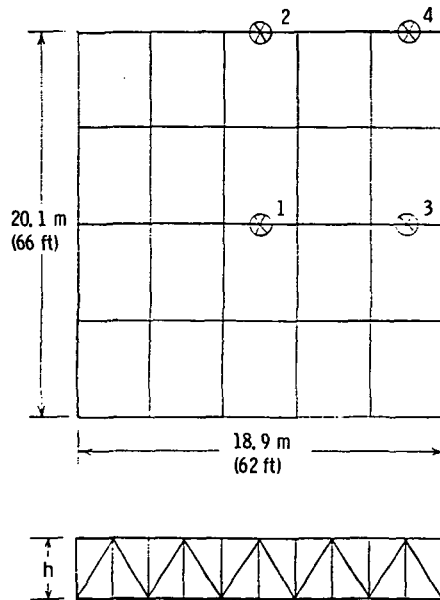


Figure 6. - Probe cart positions for movable support frame static analysis.

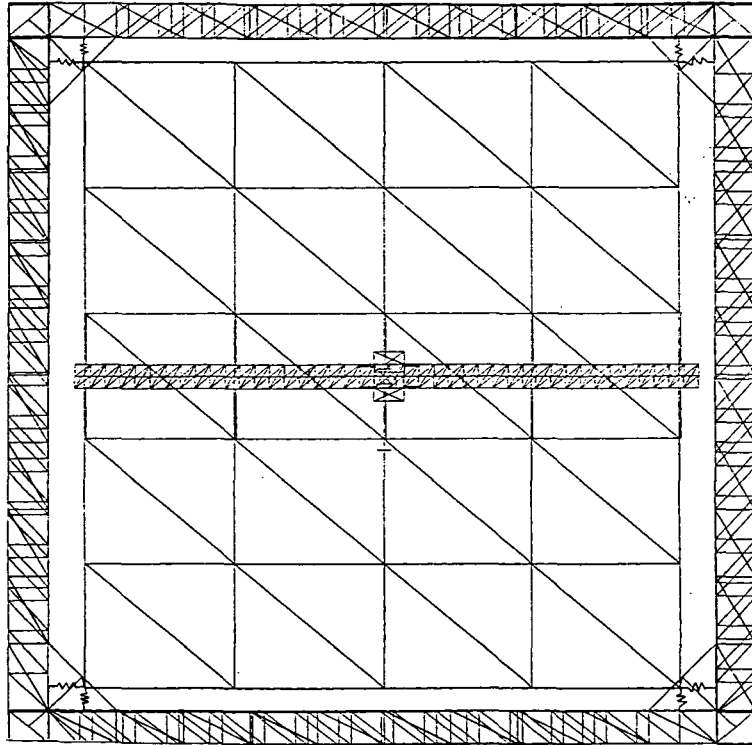


Figure 7. - Top view of simulated horizontal attachment of movable support frame to outer support frame.

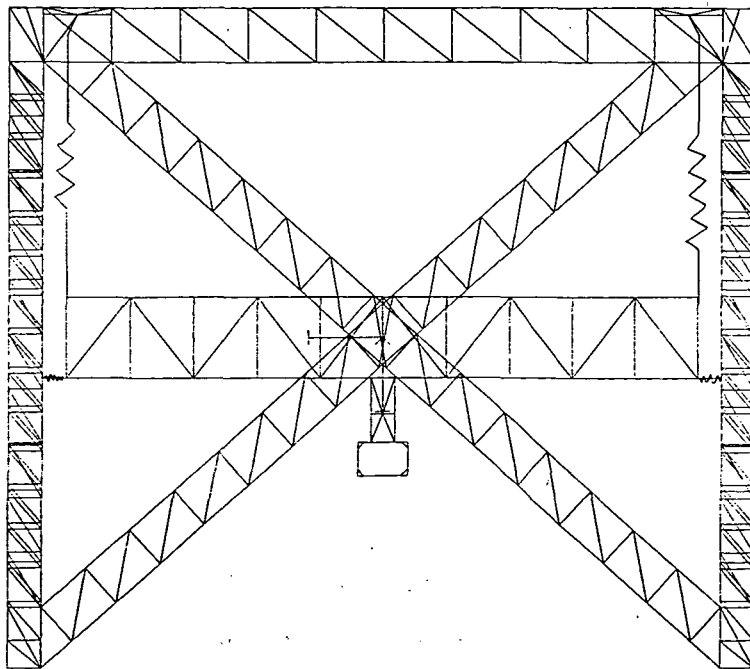


Figure 8. - Vertical drive chain and counterweight cable simulation of attachment for movable support frame; horizontal attachment simulation of movable support frame to outer support frame.

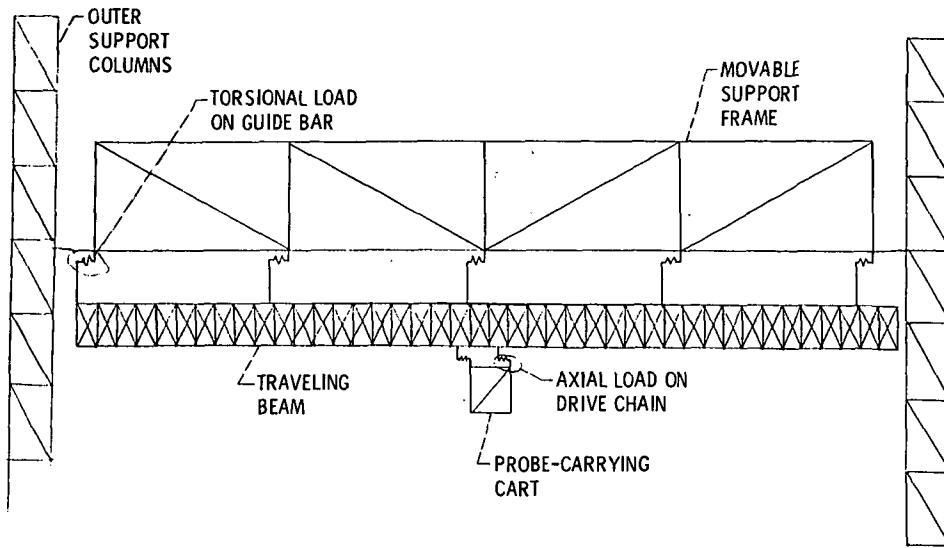


Figure 9. - Representative spring attachments of traveling beam and cart.

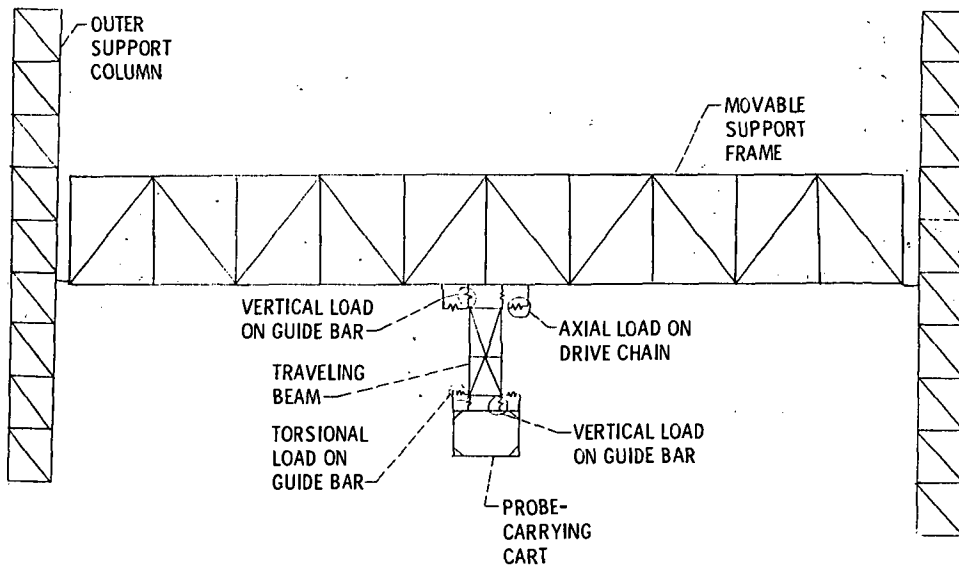


Figure 10. - Representative spring attachments of traveling beam and cart.

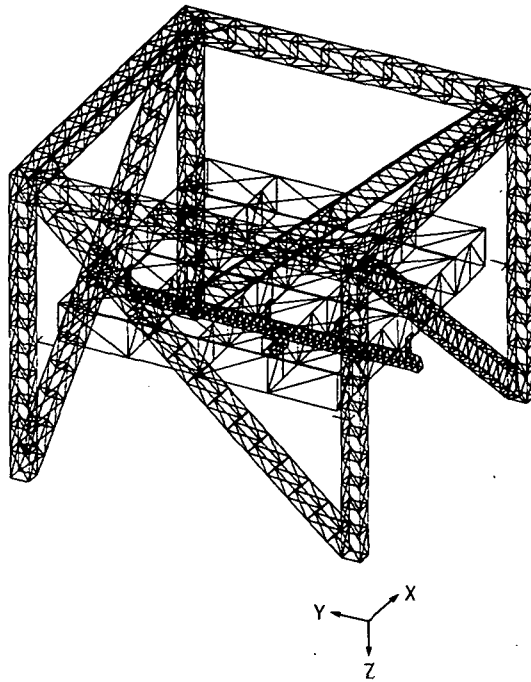


Figure 11. - NASTRAN generated model of scanner structure.

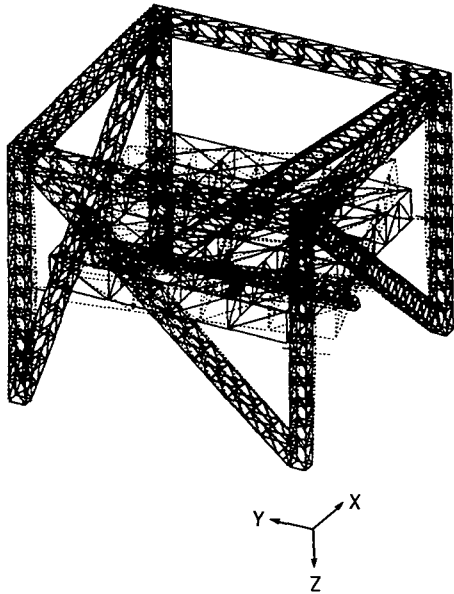


Figure 12. - Torsional mode of movable support frame about Z-Z axis. Natural frequency, 1.17 Hz.

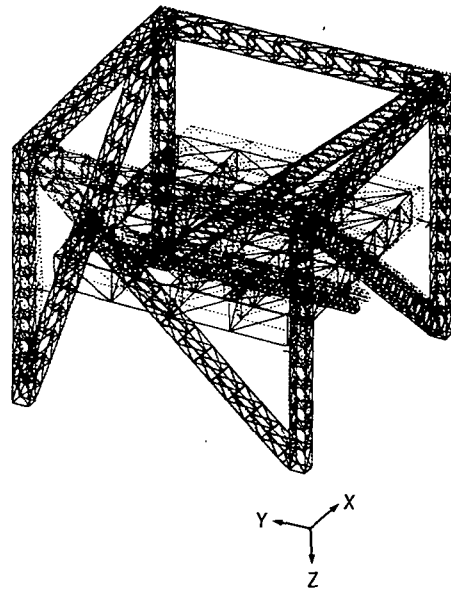


Figure 13. - Lateral mode of movable support frame along X-X axis. Natural frequency, 1.90 Hz.

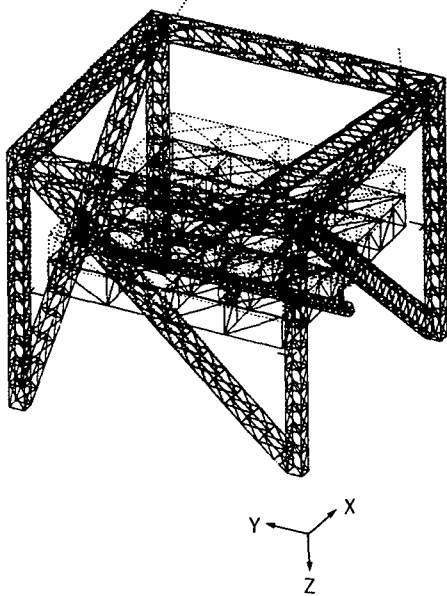


Figure 14. - Vertical mode of movable support frame along Z-Z axis. Natural frequency, 2.07 Hz.

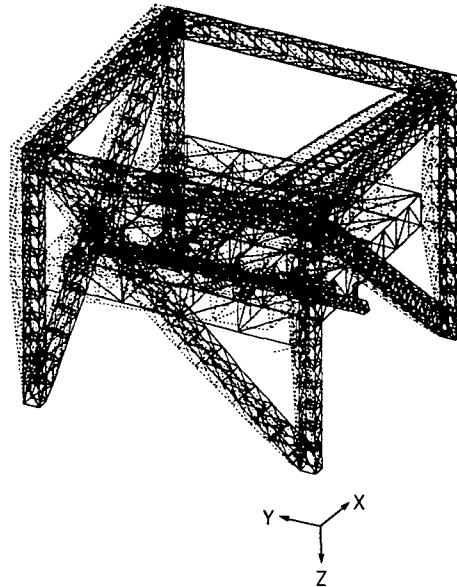


Figure 15. - Lateral mode of movable and outer support frame along Y-Y axis. Pitching of movable support frame about X-X axis. Natural frequency, 2.54 Hz.

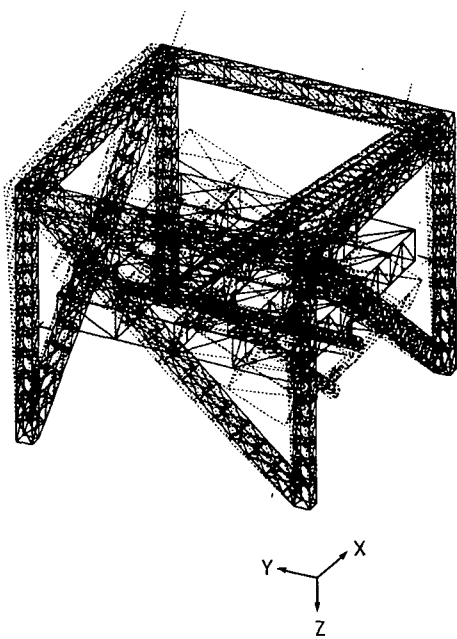


Figure 16. - Movable support frame pitching about X-X axis. Lateral mode of outer support frame along Y-Y axis. Natural frequency, 3.00 Hz

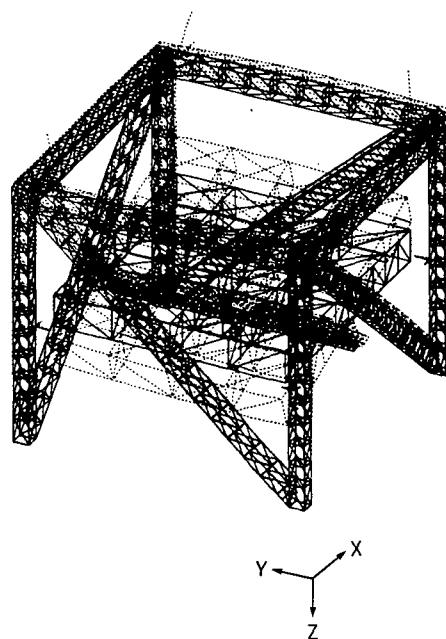
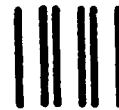


Figure 17. - Movable support frame pitching about Y-Y axis coupled with lateral bending of traveling beam. Lateral mode of outer support frame along X-X axis. Natural frequency, 3.08 Hz.

1. Report No. NASA TM-83781		2. Government Accession No.		3. Recipient's Catalog No.	
4. Title and Subtitle Structural Design of a Vertical Antenna Boresight 18.3- by 18.3-m Planar Near-Field Antenna Measurement System				5. Report Date	
				6. Performing Organization Code 506-58-22	
7. Author(s) G. Richard Sharp, Paul A. Trimarchi, and Joyce S. Wanhainen				8. Performing Organization Report No. E-2274	
				10. Work Unit No.	
9. Performing Organization Name and Address National Aeronautics and Space Administration Lewis Research Center Cleveland, Ohio 44135				11. Contract or Grant No.	
				13. Type of Report and Period Covered Technical Memorandum	
12. Sponsoring Agency Name and Address National Aeronautics and Space Administration Washington, D.C. 20546				14. Sponsoring Agency Code	
15. Supplementary Notes Prepared for the Meeting of the Antenna Measurement Techniques Association, San Diego, California, October 2-4, 1984.					
16. Abstract A large very precise near-field planar scanner has been proposed for NASA Lewis Research Center. This scanner would permit near-field measurements over a horizontal scan plane measuring 18.3 m by 18.3 m. Large aperture antennas mounted with antenna boresight vertical could be tested up to 60 GHz. When such a large near field scanner is used for pattern testing, the antenna or antenna system under test does not have to be moved. Hence, such antennas and antenna systems can be positioned and supported to simulate their configuration in zero g. Thus, very large and heavy machinery that would be needed to accurately move the antennas can be avoided. A preliminary investigation has been undertaken to address the mechanical design of such a challenging near-field antenna scanner. The configuration, structural design and results of a parametric NASTRAN structural optimization analysis are contained in this report. Further, the resulting design was dynamically analyzed in order to provide resonant frequency information to the scanner mechanical drive system designers. If other large near field scanners of comparable dimensions are to be constructed, the information in this report can be used for design optimization of these also.					
17. Key Words (Suggested by Author(s)) Near-field antenna; Instrumentation; Measurement; Large near-field antenna range facility			18. Distribution Statement Unclassified - unlimited STAR Category 35		
19. Security Classif. (of this report) Unclassified		20. Security Classif. (of this page) Unclassified		21. No. of pages	22. Price*

National Aeronautics and
Space Administration

SPECIAL FOURTH CLASS MAIL
BOOK



Washington, D.C.
20546

Official Business
Penalty for Private Use, \$300

Postage and Fees Paid
National Aeronautics and
Space Administration
NASA-451

NASA

POSTMASTER: If Undeliverable (Section 158
Postal Manual) Do Not Return
